

Relaxation of antihydrogen from Rydberg to ground state

Eric M. Bass and Daniel H. E. Dubin

Department of Physics, University of California at San Diego, La Jolla, CA USA 92093-0319

Abstract. Atoms formed in highly-magnetized, cryogenic Penning trap plasmas, such as those used in the Athena and ATRAP antihydrogen experiments, form in the guiding-center atom regime. In this regime, the positron orbit is well described by classical guiding-center drift dynamics. Electromagnetic radiation from such atoms is minimal, and energy loss is accomplished primarily through collisions between the atom and free positrons. With Fokker-Planck theory and Monte-Carlo simulation, we calculate the mean energy change an ensemble of such atoms experiences after the atom has been formed. Using this result, we show that the bulk of atoms formed in antihydrogen experiments do not relax out of the guiding-center regime to binding energies where radiation can become important.

Keywords: antihydrogen, recombination, non-neutral plasmas, guiding-center atoms

PACS: 34.80.Lx, 52.27.Jt, 34.60.+z

Current antihydrogen formation experiments pass antiprotons through a cryogenic positron plasma contained in a Penning trap [1, 2]. Bound antiproton-positron pairs are expected to form by three-body recombination, which scales favorably with decreasing temperature. The three-body recombination rate has been calculated previously [3, 4] as

$$R_3 \approx 0.07n^2\bar{v}b^5 \propto T^{-9/2}, \quad (1)$$

where n and T are the positron plasma density and temperature, respectively, $\bar{v} = \sqrt{kT/m_e}$ is the positron thermal speed, and $b = e^2/kT$ is the classical distance of closest approach. What is meant by “recombination” in this case is the formation of bound pairs at binding energies $|U|$ of a few kT . Let us define

$$\varepsilon = \frac{|U|}{kT}.$$

At $\varepsilon \approx 4$, known as the kinetic bottleneck energy, atoms are unlikely to become re-ionized by thermal collisions and should eventually cascade to the ground state. We are concerned here with the rate of this cascade. We will address the question primarily by calculating the mean energy-loss rate atoms will experience at given binding energies. We use a Fokker-Planck theory for large impact parameter collisions, in which binding energy changes are small, and address collisions at all impact parameters with a Monte-Carlo simulation.

At cryogenic temperatures, the kinetic bottleneck binding energy is only a few meV, corresponding to a quantum n number of about 30 to 35. At this high excitation level, atom orbits are well described with classical equations of motion. For guiding-center atoms, the positron’s motion is integrable, described by a superposition of cyclotron,

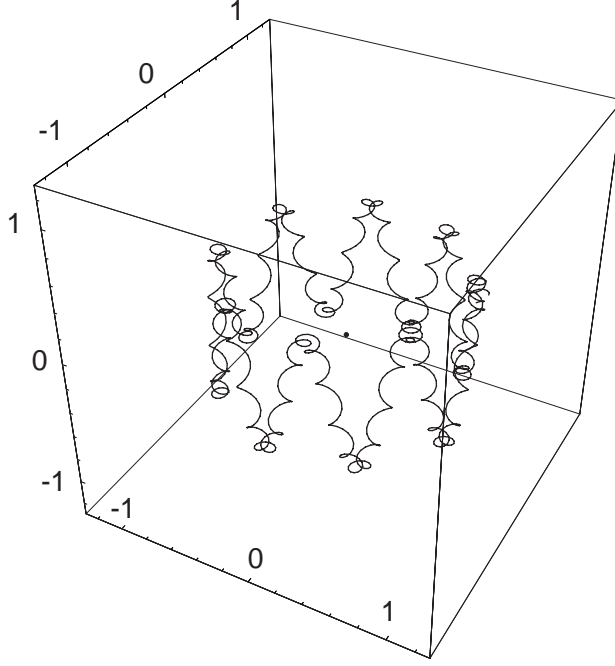


FIGURE 1. A guiding-center atom. The positron $\mathbf{E} \times \mathbf{B}$ drifts in the electric field of a stationary antiproton while oscillating back and forth along the magnetic field in the potential well of the antiproton, and performing cyclotron motion.

bounce and $\mathbf{E} \times \mathbf{B}$ drift motion. Each motion is periodic and described by a separable action-angle pair. The frequencies of these periodic motions, i.e. cyclotron, bounce, and drift (Ω_c , ω_z , and ω_ϕ respectively), obey the following ordering in guiding-center atoms:

$$\Omega_c > \omega_z > \omega_\phi. \quad (2)$$

Figure 1 shows one such guiding-center drift atom.

Let us re-scale all frequencies as

$$\hat{\omega} = \frac{b\omega}{\bar{v}}.$$

The bounce and drift frequencies ω_z and ω_ϕ scale as

$$\begin{aligned} \hat{\omega}_z &\approx \varepsilon^{3/2} \\ \hat{\omega}_\phi &\approx \frac{\varepsilon^3}{\Omega_c} \end{aligned} \quad (3)$$

When ε approaches $\hat{\Omega}_c^{2/3}$, all frequencies converge on $\hat{\Omega}_c$ and the ordering of Eq. (2) breaks down. At or near this energy, the positron orbit becomes chaotic. Fig. 2 shows one such chaotic atom.

The three oscillatory modes in the guiding-center atom each have an associated action. Considering only the guiding-center coordinates and ignoring phase, the axial bounce action I_z and the drift action I_ϕ fully specify an orbit. In the chaotic regime, the only

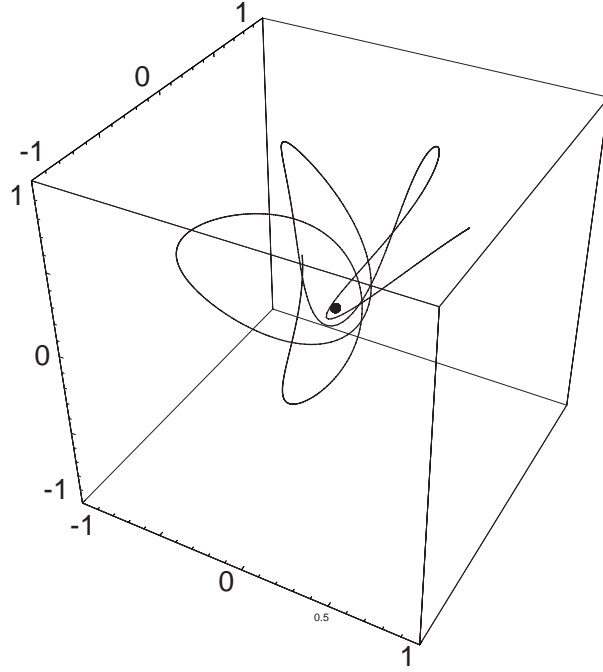


FIGURE 2. A chaotic atom. The three oscillation frequencies Ω_c , ω_z , and ω_ϕ are comparable, so energy is shared between degrees of freedom. The canonical angular momentum p_ϕ and total energy are the only constants of the motion.

constants of the motion are the total energy U and the canonical angular momentum p_ϕ . Note that, given $\frac{\partial p_\phi}{\partial t} = 0$, we have $I_\phi = 2\pi p_\phi$ for the drift orbit action.

Possible mechanisms for energy loss from guiding-center atoms include electromagnetic radiation and collisions with free positrons. The slow drift orbit of a guiding-center atom emits very little radiation, so the cascade to deep binding is accomplished through atom-positron collisions. If this cascade gets the atom near the chaotic regime $\varepsilon \gtrsim \hat{\Omega}_c^{2/3}$, radiation takes over as the dominant energy-loss mechanism. With theory and simulation, we show that an average atom takes tens of collision times to reach the chaotic regime. Since the atoms, untrapped due to their neutral charge, are expected to remain within the plasma for only a few collision times, most atoms will escape the trap in a highly-excited state. However, simulation data suggest that some small fraction may reach the chaotic regime within one collision time. Work to quantify this result is currently underway.

The simulation consists of repeated, independent collisions of thermal positrons with a guiding-center atom of binding energy ε_0 . In each run, the atom is set up in a given realization of $\varepsilon = \varepsilon_0$. First r is chosen with probability $P(r) \propto r/\omega_z$. Then, the z -axis position is chosen with probability $P_{\text{atm}}(\hat{z}) \propto 1|\hat{v}_z(\varepsilon_0, \hat{r}, \hat{z})|$. The sign of v_z (the magnitude of which is already determined) is chosen with equal probability to be positive or negative. The impacting positron's radius and angle relative to the guiding-center atom orbit are chosen with equal probability for equal area, with radius restricted

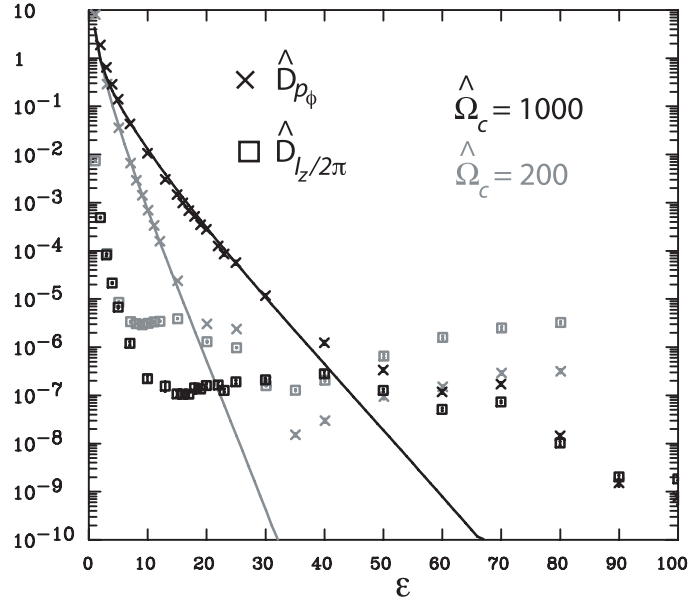


FIGURE 3. The dimensionless diffusion coefficient $\hat{D}_{p_\phi} = \frac{D_{p_\phi}}{n\bar{v}b^2(m_e\bar{v}b)^2}$, averaged over p_ϕ , is shown for $\hat{\Omega}_c=200$ and $\hat{\Omega}_c=1000$. The line is the theory from Ref. [5] and the points are moments taken from the simulation. Simulation points are also shown for D_{I_z} , for which no adequate theory exists.

to $0 < r_p < 10/\epsilon_0$. Its velocity is chosen from the distribution $P_p(\hat{v}_z) \propto |\hat{v}_z|e^{-\hat{v}_z^2/2}$. This prescription produces a physical sampling of collisions between a thermal positron plasma and an atom of given initial binding energy ϵ_0 . The collision is run using drift dynamical equations of motion unless any two of the three charges involved come within a distance of $2b/\hat{\Omega}_c^{2/3}$. In this case, cyclotron dynamics are expected to be important, and the simulation switches over to the full Newtonian equations of motion. The initial and final configurations of around 10^4 collisions were recorded at a sampling of binding energies for $\hat{\Omega}_c = 1000$ and 200 .

Let us first consider collisions with an impact parameter much larger than the atom size. Each such collision makes only a small change to atomic orbital parameters, so we can treat the energy-loss process with Fokker-Planck theory. We confine the analysis to guiding-center atoms, for which collisional energy loss dominates. Consider an ensemble of guiding-center atoms, with distribution function $f(p_\phi, I_z)$, undergoing a diffusive walk in the two orbital parameters I_z and p_ϕ down the electric potential gradient. The Fokker-Planck equation, combined with an Einstein relation, gives the flux [6].

$$\Gamma_{p_\phi} = D_{p_\phi} \left(\frac{\partial \epsilon}{\partial p_\phi} f - \frac{\partial f}{\partial p_\phi} \right) ; \quad \Gamma_{I_z} = D_{I_z} \left(\frac{\partial \epsilon}{\partial I_z} f - \frac{\partial f}{\partial I_z} \right) \quad (4)$$

D_{p_ϕ} is readily calculated theoretically given the simple, circular nature of the ϕ orbit (see Ref. [5]). The bounce motion, however, is anharmonic, and the diffusion coefficient D_{I_z} is much more difficult to determine. But, since the z coordinate oscillation is much faster than the $\mathbf{E} \times \mathbf{B}$ drift motion in ϕ , I_z is an adiabatic invariant. Therefore, we let $\Gamma_{I_z} = 0$. This argument breaks down if the frequencies ω_z and ω_ϕ are comparable, but

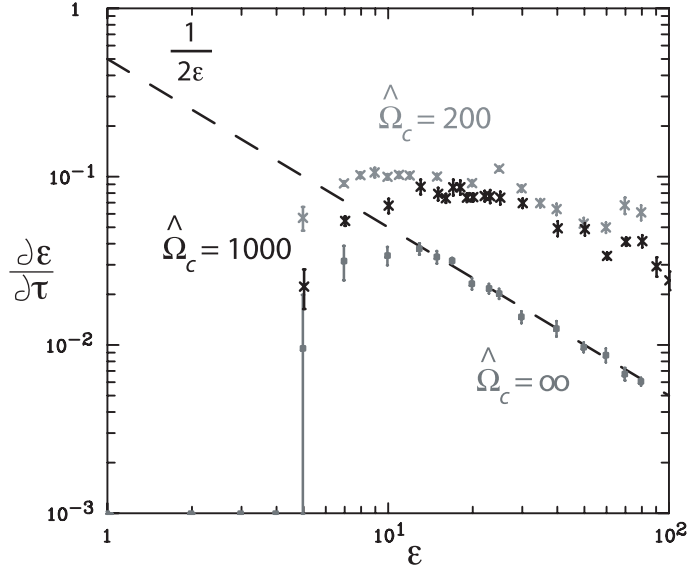


FIGURE 4. The energy-loss rate for three magnetic field strengths, parameterized by $\hat{\Omega}_c$.

for sufficiently high magnetic field our ordering holds true (see Fig. 3).

Figure 3 shows the theoretical diffusion coefficient given in Ref. [5], along with points calculated from the Monte-Carlo simulation. In the guiding-center regime, D_{p_ϕ} decreases exponentially with ε as ω_ϕ becomes large compared to the mean collision timescale \bar{v}/b , and an adiabatic invariant comes into play (Ref. [5]). The D_{I_z} values from the simulation verify a posteriori that this diffusion coefficient is small compared to D_{p_ϕ} . Note that, at large ε , the D_{p_ϕ} measured in the simulation does not drop off exponentially as expected from the theory. This is because, near the chaotic cutoff ($\varepsilon = 100$ for $\hat{\Omega}_c = 1000$ and $\varepsilon = 34.2$ for $\hat{\Omega}_c = 200$), the cyclotron frequency Ω_c takes over as the relevant frequency of motion. Since this frequency is constant, the diffusion coefficient is roughly constant as well.

We also obtain the energy-loss rate for a given binding energy ε_0 from the simulations. Figure 4 shows the mean energy-loss rate from all collisions. The $\hat{\Omega}_c = \infty$ case scales with atom cross section, but cyclotron dynamics create a more complicated scaling in the other two cases. In particular, for finite magnetic field, the rate does not vary much with magnetic field (through $\hat{\Omega}_c$). In practice, the collision frequency, by which $\partial\varepsilon/\partial\tau$ is normalized, sets the time scale for relaxation.

Figure 5 shows the time evolution of two atoms (ATRAP and Athena plasma parameters) given a fit to the collisional energy-loss rate shown in Fig. 4 added to an estimated radiative loss rate. To estimate radiative energy loss, we have averaged the classical Larmor radiative power over the energy surface, assuming that angular momentum p_ϕ takes its average value for the given binding energy. The details of this procedure will be described in a forthcoming paper. Since $\hat{\Omega}_c = 38.9$ for Athena and $\hat{\Omega}_c = 474$ for ATRAP, our collisional energy-loss data are more applicable to the later experiment. For the estimated evolutions shown, we rely on the $\hat{\Omega}_c = 200$ data points. For the most optimistic estimate of atom transit time, during which the atom can still undergo collisional energy

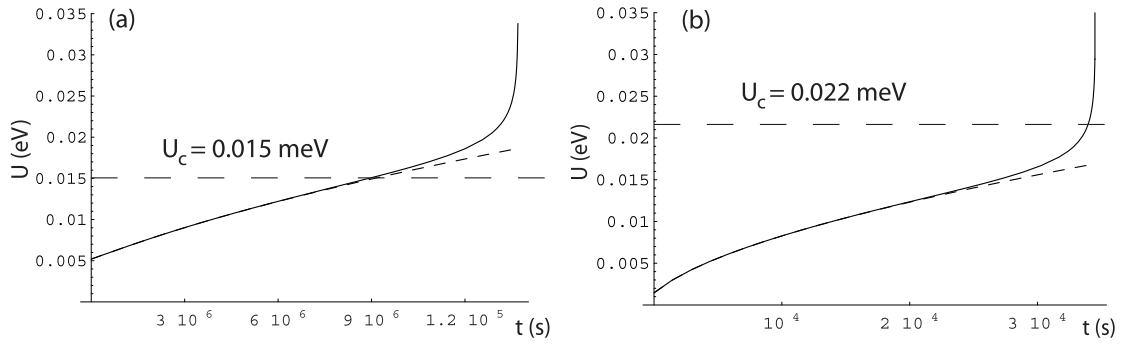


FIGURE 5. An estimated time evolution of an average guiding-center atom in the Athena plasma (a) and an ATRAP plasma (b). The dotted curve is the evolution due to collisions only. The evolution shows radiation becoming important around $10\mu\text{s}$ for Athena, and $300\mu\text{s}$ for ATRAP. The edge of the chaotic regime, U_c , is estimated with a dashed line.

loss, we assume the antiproton is near the positron thermal speed (15K for Athena, 4.2K for ATRAP). Then the transit time in the Athena plasma is between $0.3\mu\text{s}$ and $2\mu\text{s}$. For ATRAP, the time is approximately $0.1\mu\text{s}$. This is not enough time in either case for most of the atoms to reach the chaotic regime.

However, our simulations indicate that a small fraction of the particles do reach the chaotic regime quickly. Work is underway to quantify the fraction of atoms that reach a radiating regime. Once in this regime, an atom is expected to relax to the ground state quickly.

ACKNOWLEDGMENTS

The authors thank Profs. C. F. Driscoll and T. M. O’Neil for useful discussions. This work was supported by National Science Foundation Grant No. PHY0354979.

REFERENCES

1. M. Amoretti, C. Amsler, G. Bonomi et al., *Phys. Rev. Lett.* **91**, 055001 (2003).
2. G. Gabrielse, N. S. Bowden, P. Oxley et al., *Phys. Rev. Lett.* **89**, 233401 (2002).
3. Michael E. Glinsky and Thomas M. O’Neil, *Phys. Fluids B* **3**, 1279 (1991).
4. F. Robicheaux and J. D. Hanson, *Phys. Rev. A* **69**, 010701 (2004).
5. E. M. Bass and D. H. E. Dubin, *Phys. Plasmas*, 1240 (2003).
6. Frederick Reif, *Fundamentals of statistical and thermal physics*, McGraw-Hill, New York, 1965, p. 567.